

## Characteristic features of the temperature dependence of the surface impedance in polycrystalline MgB<sub>2</sub> samples

YU. A. NEFYODOV<sup>1</sup>, M. R. TRUNIN<sup>1</sup>, A. F. SHEVCHUN<sup>1</sup>,  
D. V. SHOVKUN<sup>1</sup>, N. N. KOLESNIKOV<sup>1</sup>, M. P. KULAKOV<sup>1</sup>,  
A. AGLIOLO GALLITTO<sup>2</sup> and S. FRICANO<sup>2</sup>

<sup>1</sup> *Institute of Solid State Physics - 142432 Chernogolovka, Moscow district, Russia*

<sup>2</sup> *INFM, Unità di Palermo and Dipartimento di Scienze Fisiche e Astronomiche  
Via Archirafi 36, I-90123 Palermo, Italy*

(received 13 November 2001; accepted in final form 4 February 2002)

PACS. 74.25.Nf – Response to electromagnetic fields (nuclear magnetic resonance, surface impedance, etc.).

PACS. 74.70.Ad – Metals; alloys and binary compounds (including A15, Laves phases, etc.).

**Abstract.** – The real  $R_s(T)$  and imaginary  $X_s(T)$  parts of the surface impedance  $Z_s(T) = R_s(T) + iX_s(T)$  in polycrystalline MgB<sub>2</sub> samples of different density with the critical temperature  $T_c \approx 38$  K are measured at the frequency of 9.4 GHz and in the temperature range  $5 \leq T < 200$  K. The normal skin-effect condition  $R_s(T) = X_s(T)$  at  $T \geq T_c$  holds only for the samples of the highest density with roughness sizes not more than  $0.1 \mu\text{m}$ . For such samples extrapolation  $T \rightarrow 0$  of the *linear* at  $T < T_c/2$  temperature dependences  $\lambda_L(T) = X_s(T)/\omega\mu_0$  and  $R_s(T)$  results in values of the London penetration depth  $\lambda_L(0) \approx 600 \text{ \AA}$  and residual surface resistance  $R_{\text{res}} \approx 0.8 \text{ m}\Omega$ . In the entire temperature range the dependences  $R_s(T)$  and  $X_s(T)$  are well described by the modified two-fluid model.

The inconclusive situation with the mechanism of superconductivity in MgB<sub>2</sub> [1] is mainly due to the lack of consensus on many important physical quantities in this material. For example, the energy gap ratio  $2\Delta/kT_c$  ranging from 1 to 5 has been reported, which raises the possibility of an anisotropic energy gap or a multiple gap. Indeed, recent tunneling [2] and point contact [3] experiments showed two distinct conductance peaks of different magnitude, and to describe the specific heat data [4] the authors involved either two gaps or an anisotropic gap. At the same time a number of high-frequency measurements in MgB<sub>2</sub> films found a small single gap (the gap ratio is well below the weak-coupling value) if the data was fitted by BCS model with isotropic *s*-wave order parameter [5–8]. In particular, the exponential temperature dependence of the magnetic-field penetration depth at  $T \ll T_c$  gave occasion to such fitting [7, 8]. However, in very dense polycrystalline MgB<sub>2</sub> samples the linear  $\Delta\lambda(T) \propto T$  behavior was observed [9, 10]. Other measurements in MgB<sub>2</sub> powders and ceramics provided rather contradictory results:  $\Delta\lambda(T)$ -dependences were proportional to  $T$  (ref. [11]),  $T^2$  (ref. [12]),  $T^{2.7}$  (ref. [13]) and  $\exp[-\Delta/T]/T^{0.5}$  (ref. [14]). The estimated values of  $\lambda(0)$  varied from as low as 85 nm in ref. [12] up to 300 nm in ref. [6]. Apparently, the data spread indicates that the measured parameters of MgB<sub>2</sub> depend on the sample quality and growth technique. Nevertheless, it is generally accepted that in the *ab*-plane of MgB<sub>2</sub> the coherence length  $\xi_0$  does not exceed  $100 \text{ \AA}$  and, hence, MgB<sub>2</sub> samples characterized by the value of electron relaxation

rate  $1/\tau(T_c) < 10^{13} \text{ s}^{-1}$  (the mean free path  $l > 500 \text{ \AA}$ ) should be classified as London ( $\xi_0 \ll \lambda$ ) pure ( $l \gg \xi_0$ ) superconductors.

Microwave measurements of the surface impedance temperature dependences  $Z_s(T) = R_s(T) + iX_s(T)$  provide accurate determination of applied and fundamental parameters of the superconducting state (residual surface resistance  $R_{\text{res}} \equiv R_s(T \rightarrow 0)$ , superconducting gap and its symmetry, penetration depth) and normal state (normal or anomalous skin-effect, resistivity  $\rho$ , relaxation rate). At the frequency of 10 GHz the skin depth  $\delta = \sqrt{2\rho/\omega\mu_0} > 1 \mu\text{m}$  is much greater than  $l$  in  $\text{MgB}_2$  and, therefore, at  $T \geq T_c$  the criterion of the normal skin-effect should apply:

$$R_s(T) = X_s(T) = \rho(T)/\delta(T) = \sqrt{\omega\mu_0\rho(T)/2}. \quad (1)$$

Equation (1) follows from the general relation between the impedance and conductivity ( $\sigma = \sigma_1 - i\sigma_2$ ) components in London superconductors:

$$R_s = \sqrt{\frac{\omega\mu_0(\varphi^{1/2} - 1)}{2\sigma_2\varphi}}, \quad X_s = \sqrt{\frac{\omega\mu_0(\varphi^{1/2} + 1)}{2\sigma_2\varphi}}, \quad (2)$$

where  $\varphi = 1 + (\sigma_1/\sigma_2)^2$ . It is obvious that  $R_s \leq X_s$ . As follows from eq. (2) in the immediate vicinity of the transition temperature there is a very narrow peak in the curve  $X_s(T)$ . When  $(\sigma_1/\sigma_2)^2 \ll 1$ , which is valid at temperatures not very close to  $T_c$ , where the magnetic-field penetration depth  $\lambda = \sqrt{1/\omega\mu_0\sigma_2}$ , from eq. (2) we get  $R_s \approx \omega^2\mu_0^2\sigma_1\lambda^3/2$  and  $X_s \approx \omega\mu_0\lambda$ . In pure London superconductor the value of  $\lambda$  is the London penetration depth which equals  $\lambda_L(0) = m/\mu_0ne^2$  at  $T = 0$ .

In the centimeter wavelength band the surface resistance  $R_s(T)$  was measured in  $\text{MgB}_2$  wire [15], pellets [10, 15], separated grains [16], and films [7, 11, 17]. The value of  $R_{\text{res}}$  characterizing the sample quality was proved to be highly dependent on the sample preparation and processing. The transformed ( $\propto \omega^2$ ) to the same frequency 10 GHz values of  $R_{\text{res}}$  varied from 0.7 to 5 m $\Omega$  in different  $\text{MgB}_2$  bulk samples [7, 11, 15–17] except the wire [15] where the lower-range  $R_{\text{res}} \approx 0.1 \text{ m}\Omega$  is found. However, in all previous publications devoted to microwave investigations of  $\text{MgB}_2$  there had been no data on the  $X_s(T)$  in absolute units, which means that eq. (1) applicability was not verified nor was the value of  $\lambda(0) = X_s(0)/\omega\mu_0$  determined directly from microwave measurements of  $\text{MgB}_2$ .

In this letter, we present precise measurements of the real and imaginary parts of the surface impedance in polycrystalline  $\text{MgB}_2$  samples of different porosity. We found that normal skin-effect condition  $R_s(T) = X_s(T)$  at  $T \geq T_c$  holds only for the samples of the highest (close to theoretical) density. For such samples the electrodynamic parameters of the normal and superconducting state of  $\text{MgB}_2$  are obtained.

The samples investigated were synthesized *in situ* from amorphous boron powder and lump metal magnesium, both with purity better than 99.96%. Two types of different  $\text{MgB}_2$  polycrystalline bulk samples were investigated. The samples of the first type were synthesized at 1100 °C with subsequent rapid cooling, and the samples of the second type were obtained after heating  $\text{MgB}_2$  up to 1400 °C and then keeping this temperature for an hour (for details see ref. [18]). Using a diamond circular saw we cut small thin plates ( $\sim 1 \times 1 \times 0.1 \text{ mm}^3$ ) from the obtained compact ceramic cylinders and polished their surfaces using fine ( $\sim 0.1 \mu\text{m}$ ) diamond powder diluted by the high-purity benzine (ethanol initially used for this purpose resulted in large microwave absorption of the sample). After polishing and cleaning, the samples were being heated at 200 °C for 4 hours in high vacuum. The average grain size of about  $\sim 20 \mu\text{m}$  and density of 2.52 g/cm<sup>3</sup> were obtained for the samples of the first type and the corresponding values of  $\sim 40 \mu\text{m}$  and 2.23 g/cm<sup>3</sup> for the samples of the second type. This density drop was

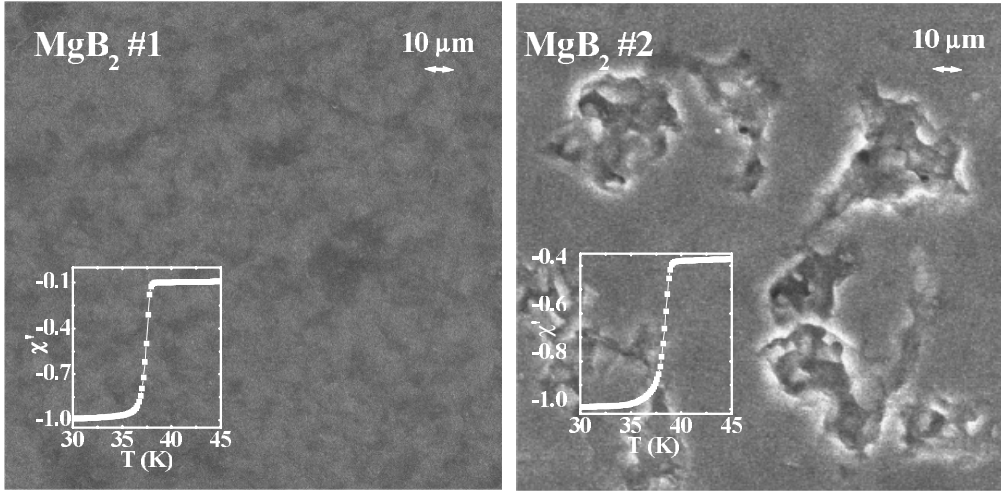


Fig. 1 – SEM micrographs of the sample #1 (a) and #2 (b) in the same scale. The insets show the  $\chi'(T)$  curves of these samples in the vicinity of the superconducting transition.

due to Mg-evaporation resulting in numerous small voids (5–30 microns) in the ceramics. This can be seen in fig. 1, where scanning electron micrographs (second-electron emission mode) of the samples #1 and #2 are shown. Sample #1 belongs to the first type (dimensions:  $1.34 \times 1.10 \times 0.03 \text{ mm}^3$ ) and sample #2 is of the second type ( $1.57 \times 1.56 \times 0.22 \text{ mm}^3$ ). Unlike sample #2 the surface of the densest sample #1 looks homogeneous, at least the dimensions of possible irregularities are less than scanning resolution of  $0.1 \mu\text{m}$ .

Preliminary testing of MgB<sub>2</sub> samples was carried out with the aid of the temperature measurements of their dynamic susceptibility  $\chi(T) = \chi'(T) - i\chi''(T)$  performed by a four-coil scheme at 100 kHz. The insets in fig. 1 show very similar temperature dependences of the shielding  $\chi'(T)$  of the magnetic field in both samples. If the penetration depth  $\lambda(T) = \lambda(0) + \Delta\lambda(T)$  is much smaller than the characteristic size  $a$  (which is the size of either the sample or grains in it), then at low temperatures  $T < T_c$  the dependence  $\chi'(T)$  corresponds to the  $\lambda(T)$  variation:  $\chi'(T) = \chi'_0(1 - \Delta\lambda(T)/a)$ .

For the measurements at 9.4 GHz we applied the “hot-finger” technique which had been used to characterise the microwave properties of small crystals of high- $T_c$  and conventional superconductors [19]. The temperature dependences of the  $Q$ -factor,  $Q^{-1} \propto R_s$ , and the frequency shift  $\Delta f \propto \Delta X_s$  of the cavity with the sample inside are measured simultaneously. To determine  $R_s(T)$  and  $X_s(T)$  in absolute units one needs to know the value of the sample geometrical factor  $\Gamma$  and the constant  $X_0 = X_s(T) - \Delta X_s(T)$ . The parameter  $\Gamma$  can be determined both empirically and theoretically and its value depends on the shape and dimensions of the sample and its position in the cavity with respect to the microwave field  $\mathbf{H}_\omega$  [19]. The constant  $X_0$  can be derived from the condition of equality between the real and imaginary parts of the normal-state surface impedance. Temperature dependences of the surface resistance (open squares) and reactance (open circles) in both samples are shown in fig. 2.  $Z_s(T)$  curves measured in the field  $\mathbf{H}_\omega$  perpendicular and parallel to the biggest faces of the sample were identical. The resistivity  $\rho(T_c) = 2R_s^2(T_c)/\mu_0\omega$  obtained from the surface resistance value  $R_s(T_c)$  is equal to  $8 \mu\Omega\text{cm}$  and  $15 \mu\Omega\text{cm}$  for samples #1 and #2, respectively. The measured value of  $T_c \approx 38 \text{ K}$  and the residual resistivity ratio  $\text{RRR} = \rho(300 \text{ K})/\rho(T_c) \approx 3$  for both samples corresponds to the nominal composition Mg:B = 1:2 (refs. [20, 21]).

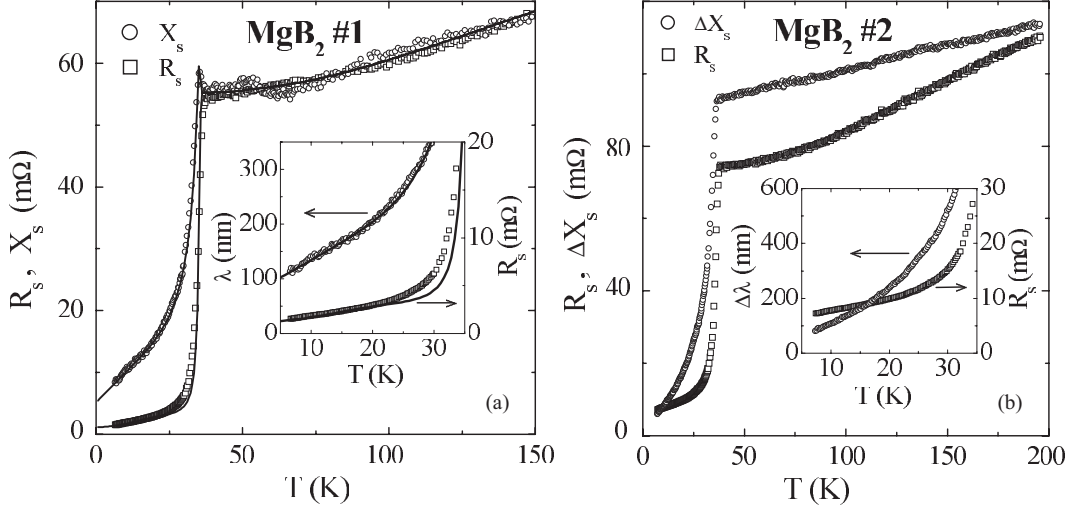


Fig. 2 – Plots of the surface resistance  $R_s(T)$  and reactance  $X_s(T)$  at 9.4 GHz in MgB<sub>2</sub> samples #1 (a) and #2 (b). The insets show the low-temperature sections of  $R_s(T)$  and London penetration depth  $\lambda_L(T) = X_s(T)/\omega\mu_0$ . The solid curves in fig. 2(a) show calculations based on the modified two-fluid model.

Essential distinction in samples #1 and #2 appears in their  $\Delta X_s(T)$ -dependences. Whereas the sample #1 parameters are in accordance with eqs. (1), (2):  $R_s(T) = X_s(T)$  at  $T \geq T_c$ , and  $\Delta X_s(T) < \Delta R_s(T)$  at  $T < T_c$ , the sample #2 reactance variation  $\Delta X_s(T)$  is considerably larger than that of the resistance  $\Delta R_s(T)$  in the entire temperature range. Unusually large change  $\Delta X_s(T) > \Delta R_s(T)$  was previously reported in the microwave *ab*-response of Tl<sub>2</sub>Ba<sub>2</sub>CuO<sub>6+δ</sub> single crystals [22–24]. As a possible explanation in ref. [23] it was proposed to allow for the shielding effect of the microwave field by roughnesses (cleavage plane traces) of Tl<sub>2</sub>Ba<sub>2</sub>CuO<sub>6+δ</sub> crystal surface. If the penetration depth is much less than roughness sizes, both components of the effective surface impedance measured will increase in comparison with their values for a flat surface by the same factor equal to the ratio of the real and flat surface areas. If the roughness sizes are comparable to the penetration depth the situation may occur when  $\mathbf{H}_\omega$  is slightly distorted by the roughness, whereas the high-frequency current caused by the field decays noticeably [25]. In this case the effective reactance ( $\sim \omega\mu_0 \int H_\omega^2 dV$ ) will exceed the sample surface resistance ( $\sim \int j_\omega^* E_\omega dV$ ). It is likely that this is the case in MgB<sub>2</sub> sample #2 whose pores' dimensions proved to be comparable with its skin depth.

Another non-trivial feature of  $Z_s(T)$  curves in fig. 2 is the linear temperature dependence of both impedance components at  $T < T_c/2$  (see the insertions in fig. 2). Figure 3 demonstrates an agreement of the temperature dependences  $\Delta\lambda(T) \propto T$  measured at the frequencies 9.4 GHz and 100 kHz. Characteristic sizes  $a = \Delta\lambda(T)/\Delta\lambda'(T)$ , determined for the samples #1 and #2 with  $\chi'_0 = -1$ , proved to be equal to the average grain sizes, respectively. In the sample #1 at  $T < T_c/2$  the slopes of  $R_s(T)$  and  $X_s(T)$  curves are roughly half of that of the sample #2. In particular, the value of  $d\lambda/dT \approx 70 \text{ \AA}/\text{K}$  at  $T \ll T_c$  for the sample #1 so we can derive the value of  $\lambda_L(0) = 600 \pm 100 \text{ \AA}$ . Extrapolation  $R_s(T \rightarrow 0)$  gives  $R_{\text{res}} \approx 0.8 \text{ m}\Omega$  in this sample. The strong slope of the linear sections of  $\Delta\lambda(T)$  curves in very dense polycrystalline MgB<sub>2</sub> samples was also found in refs. [9, 10]. The above value of  $\lambda_L(0)$  is smaller than the one found previously in microwave investigations of MgB<sub>2</sub>. One should notice that elsewhere the values of  $\lambda(0)$  were obtained as a result of fitting of the measured  $\Delta\lambda(T)$  curve by the model

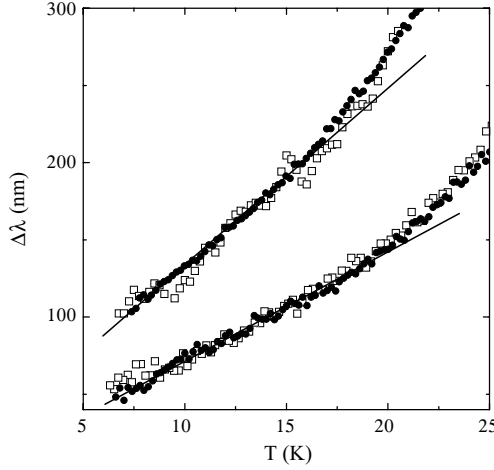


Fig. 3 – Comparison of  $\Delta\lambda(T)$  data at 9.4 GHz (black circles) and at 100 kHz (open squares) in  $\text{MgB}_2$  samples #1 and #2. The upper graph is shifted by 20 nm up for clarity.

dependence of  $\lambda(T)$ , whereas we obtain the  $\lambda_L(0)$  value directly from the measurements of  $X_s(0)$ .

Interestingly,  $R_s(T)$  and  $X_s(T)$  curves in fig. 2(a) are very similar to those measured in electron high- $T_c$  crystal  $\text{Ba}_{0.6}\text{K}_{0.4}\text{BiO}_3$  [26]. Moreover, the similarity of the optical constants in  $\text{MgB}_2$  and  $\text{Ba}_{0.6}\text{K}_{0.4}\text{BiO}_3$  was pointed out in ref. [27]. So far there is no microscopic theory explaining such a strong slope of the linear  $Z_s(T)$ -temperature-dependence at  $T$  up to  $T_c/2$  for these crystals. As early as in the old ref. [26] a modified two-fluid model (MTFM) was suggested and then developed in refs. [28] to describe  $Z_s(T)$  in all optimum doped high- $T_c$  single crystals. This phenomenological model has two essential features different from the well-known Gorter-Casimir (GC) model [29]. The former is the unique density of superconducting electrons which gives rise to a linear temperature dependence of the penetration depth at low temperatures, and the latter is the introduction of the temperature dependence of the quasi-particle relaxation time  $\tau(T)$  described by Grüneisen formula (electron-phonon interaction) with retaining the temperature-independent impurity relaxation time  $\tau(0)$ , which is present in the GC model:

$$\frac{1}{\tau} = \frac{1}{\tau(0)} \left[ 1 + \frac{t^5 \mathcal{J}_5(\kappa/t) / \mathcal{J}_5(\kappa)}{\beta} \right],$$

$$\mathcal{J}_5(\kappa/t) = \int_0^{\kappa/t} \frac{z^5 e^z dz}{(e^z - 1)^2}, \quad (3)$$

where  $t \equiv T/T_c$ ,  $\kappa = \Theta/T_c$  ( $\Theta$  is the Debye temperature), and  $\beta$  is a numerical parameter. From eq. (3) we have  $\beta = \tau(T_c)/[\tau(0) - \tau(T_c)]$ ;  $\beta \approx \tau(T_c)/\tau(0) \ll 1$  if  $\tau(0) \gg \tau(T_c)$ , and  $\beta \gg 1$  if  $\tau(0) \approx \tau(T_c)$ . The second summand in the brackets in eq. (3) is proportional to  $T^5$  at  $T < \Theta/10$  and to  $T$  at  $T > \Theta/5$ . The solid line at  $T \geq T_c$  in fig. 2(a) shows the calculation result of  $R_s(T) = X_s(T)$  from eq. (1) with parameters  $\beta = 350$  and  $\kappa = 15$  ( $\Theta \sim 600$  K) in eq. (3) for  $1/\tau(T) \propto \rho(T)$ . In the framework of MTFM the value of  $\tau(T_c) = X_s^2(0)/2\omega R_s^2(T_c) \approx 0.6 \cdot 10^{-13}$  s,  $\tau(0) = dR_s/\omega dX_s|_{T \rightarrow 0} \approx 6.6 \cdot 10^{-13}$  s (obtained using the measured slopes  $dR_s/dT$  and  $dX_s/dT$  at  $T \ll T_c$ ), and, hence,  $\beta = 0.1$  in eq. (3) for the superconducting state of sample #1. The solid lines at  $T \leq T_c$  in fig. 2(a) show the components  $R_s(T)$  and  $X_s(T)$

calculated from eq. (2). Thus,  $Z_s(T)$ -dependences measured in MgB<sub>2</sub> are well described in the framework of MTFM in the entire temperature range with the same free parameter  $\kappa = 15$  in eq. (3), but with substantially different  $\beta$  in the normal and superconducting state. As in the case with high- $T_c$  crystals, in MgB<sub>2</sub> the relaxation rate of normal carriers decreases rapidly ( $\propto T^5$ ) with decrease of temperature lower than  $T_c$ . In principle, there is a possibility to describe the linear temperature dependences of  $R_s(T)$  and  $X_s(T)$  at low  $T$  in terms of the weak-links model [30]. However, we did not observe any manifestation of intergranular weak links in our measurements of ac-susceptibility in a weak magnetic field. Moreover, magnetization [31], transport [32] and non-resonant microwave absorption [33] measurements show that MgB<sub>2</sub> does not exhibit weak-link electromagnetic behavior.

In conclusion, we state that the measurement results of the microwave surface impedance components in polycrystalline MgB<sub>2</sub> samples depend on their quality and preparation technique. The normal skin-effect criterion  $R_s(T) = X_s(T)$  at  $T \geq T_c$  is met only in very dense homogeneous samples of the highest quality characterized by the lower-range values of residual losses, superconducting transition width, and resistivity in the normal state. For these samples the values of  $\tau(T_c) \approx 10^{-13}$  s,  $\lambda_L(0) \approx 600$  Å and  $R_s(0) \approx 0.8$  mΩ are obtained directly from  $R_s(T)$  and  $X_s(T)$  measurements in absolute units. The linear dependences  $\Delta\lambda(T) \propto T$  and  $R_s(T) \propto T$  at  $T < T_c/2$  are observed. The curves  $\Delta\lambda(T)$  measured at 9.4 GHz coincide with ac-susceptibility measurements at five orders smaller frequency.  $R_s(T)$  and  $X_s(T)$  curves in the normal and superconducting state are well described in the framework of the phenomenological approach based on the usage of eq. (3) for quasiparticle scattering on impurities and phonons.

\* \* \*

This research has been supported by RFBR grant 00-02-17053, DFG-RFBR grant 00-02-04021, Scientific Council on Superconductivity (project 96060), and University of Palermo (grant Coll. Int. Li Vigni).

## REFERENCES

- [1] NAGAMATSU J., NAKAGAWA N., MURANAKA T., ZENITANI Y. and AKIMITSU J., *Nature*, **63** (2001) 410.
- [2] GIUBILEO F., RODITCHEV D., SACKS W., LAMY R., THANH D. X., KLEIN J., MIRAGLIA S., FRUCHART D., MARCUS J. and MONOD PH., *Phys. Rev. Lett.*, **87** (2001) 177008.
- [3] SZABO P., SAMUELY P., KACMARCIC J., KLEIN TH., MARCUS J., FRUCHART D., MIRAGLIA S., MARCENAT C. and JANSEN A. G. M., *Phys. Rev. Lett.*, **87** (2001) 137005.
- [4] JUNOD A., WANG Y., BOUQUET F. and TOULEMONDE P., cond-mat/0106394; BOUQUET F., FISHER R. A., PHILLIPS N. E., HINKS D. G. and JORGENSEN J. D., *Phys. Rev. Lett.*, **87** (2001) 047001.
- [5] JUNG J. H., KIM K. W., LEE H. J., KIM M. W., NOH T. W., KANG W. N., KIM HYEONG-JIN, CHOI EUN-MI, JUNG C. U. and LEE SUNG-IK, cond-mat/0105180.
- [6] KAINDL R. A., CARNAHAN M. A., ORENSTEIN J., CHEMLA D. S., CHRISTEN H. M., ZHAI H.-Y., PARANTHAMAN M. and LOWNDES D. H., cond-mat/0106342.
- [7] KLEIN N., JIN B. B., SCHUBERT J., SCHUSTER M., YI H. R., PIMENOV A., LOIDL A. and KRASNOSVOBODTSEV S. I., cond-mat/0107259.
- [8] LAMURA G., DI GENNARO E., SALLUZZO M., ANDREONE A., COCHEC J. LE, GAUZZI A., CANTONI C., PARANTHAMAN M., CHRISTEN D. K., CHRISTEN H. M., GIUNCHI G. and CERESARA S., preprint.
- [9] LI S. L., WEN H. H., ZHAO Z. W., NI Y. M., REN Z. A., CHE G. C., YANG H. P., LIU Z. Y. and ZHAO Z. X., *Phys. Rev. B*, **64** (2001) 094522.

- [10] DULCIC A., PAAR D., POZEK M., WILLIAMS G. V. M., KRAMER S., JUNG C. U., PARK MIN-SEOK and LEE SUNG-IK, cond-mat/0108071.
- [11] ZHUKOV A. A., COHEN L. F., PURNELL A., BUGOSLAVSKY Y., BERENOV A., MACMANUS-DRISCOLL J. L., ZHAI H. Y., CHRISTEN HANS M., PARANTHAMAN MARIAPPAN P., LOWNDES DOUGLAS H., JO M. A., BLAMIRE M. C., HAO LING and GALLOP J., cond-mat/0107240.
- [12] PANAGOPOULOS C., RIANFORD B. D., XIANG T., SCOTT C. A., KAMBARA M. and INOUE I. H., *Phys. Rev. B*, **64** (2001) 094514.
- [13] CHEN X. H., XUE Y. Y., MENG R. L. and CHU C. W., cond-mat/0103029.
- [14] MANZANO F. and CARRINGTON A., cond-mat/0106166.
- [15] HAKIM N., PARIMI P. V., KUSKO C., SRIDHAR S., CANFIELD P. C., BUD'KO S. L. and FINNEMORE D. K., *Appl. Phys. Lett.*, **17** (2001) 4160.
- [16] ZHUKOV A. A., YATES K., PERKINS G. K., BUGOSLAVSKY Y., POLICHETTI M., BERENOV A., DRISCOLL J., CAPLIN A. D., COHEN L. F., HAO L. and GALLOP J., *Supercond. Sci. Technol.*, **14** (2001) L13.
- [17] LEE S. Y., LEE J. H., LEE JUNG H., RYU J. S., LIM J., MOON S. H., LEE H. N., KIM H. G. and OH B., cond-mat/0105327.
- [18] KOLESNIKOV N. N. and KULAKOV M. P., *Physica C*, **363** (2001) 166.
- [19] TRUNIN M. R., *J. Supercond.*, **11** (1998) 381.
- [20] CHEN X. H., WANG Y. S., XUE Y. Y., MENG R. L., WANG Y. Q. and CHU C. W., cond-mat/0107154.
- [21] INDENBOM M. V., USPENSKAYA L. S., KULAKOV M. P., BDIKIN I. K. and ZVER'KOV S. A., *JETP Lett.*, **74** (2001) 274.
- [22] WALDRAM J. R., BROUN D. M., MORGAN D. C., ORMENO R. and PORCH A., *Phys. Rev. B*, **59** (1999) 1528.
- [23] TRUNIN M. R., *JETP Lett.*, **72** (2000) 583.
- [24] KUSKO C., ZHAI Z., HAKIM N., MARKIEVICZ R. S., SRIDHAR S., COLSON D., VIALLET-GUILLEN V., NEFYODOV YU. A., TRUNIN M. R., KOLESNIKOV N. N., MAIGNAN A. and ERB A., submitted to *Phys. Rev. Lett.*
- [25] MENDE F. F. and SPITSYN A. A., *Surface Impedance of Superconductors* (Naukova dumka, Kiev) 1985.
- [26] TRUNIN M. R., ZHUKOV A. A., TSYDYNZHAPOV G. E., SOKOLOV A. T., KLINKOVA L. A. and BARKOVSKII N. V., *JETP Lett.*, **64** (1996) 832.
- [27] TU J. J., CARR G. L., PEREBEINOS V., HOMES C. C., STRONGIN M., ALLEN P. B., KANG W. N., CHOI E. M., KIM H. J. and LEE SUNG-IK, cond-mat/0107349.
- [28] FINK H. J., *Phys. Rev. B*, **58** (1998) 9415; **61** (2000) 6346; TRUNIN M. R., NEFYODOV YU. A. and FINK H. J., *Sov. Phys. JETP*, **91** (2000) 801; FINK H. J. and TRUNIN M. R., *Phys. Rev. B*, **62** (2000) 3046.
- [29] GORTER C. S. and CASIMIR H., *Phys. Z.*, **35** (1934) 963.
- [30] HALBRITTER J., *J. Supercond.*, **8** (1995) 691.
- [31] LARBALESTIER D. C., RIKEL M. O., COOLEY L. D., POLYANSKII A. A., JIANG J. Y., PATNAIK S., CAI X. Y., FELDMANN D. M., GUREVICH A., SQUITIERI A. A., NAUS M. T., EOM C. B., HELLSTROM E. E., CAVA R. J., REGAN K. A., ROGADO N., HAYWARD M. A., HE T., SLUSKY J. S., KHALIFAH P., INUMARU K. and HAAS M., *Nature*, **410** (2001) 186.
- [32] KANG W. N., KIM KIJOON H. P., KIM HYEONG-JIN, CHOI EUN-MI, PARK MIN-SEOK, KIM MUN-SEOG, DU ZHONGLIAN, JUNG CHANG UK, KIM KYUNG HEE, LEE SUNG-IK and MUN MI-OCK, cond-mat/0103161.
- [33] JOSHI JANHAVI P., SARANGI SUBHASIS, SOOD A. K., BHAT S. V. and PAL DILIP, cond-mat/0103369.